

Supporting information for “Temperature dependence of the spectral line-width of charge transfer state emission in organic solar cells; static vs. dynamic disorder”

Kristofer Tvingstedt*, Johannes Benduhn and Koen Vandewal.

[*ktvingstedt@physik.uni-wuerzburg.de](mailto:ktvingstedt@physik.uni-wuerzburg.de)

1. Experimental section

1.1 Device manufacturing

The layers of the low-donor-content OSCs were thermally evaporated at ultrahigh vacuum (base pressure $<10^{-7}$ mbar) on a glass substrate with a pre-structured ITO contact (Thin Film Devices). For an appropriate hole contact 2nm of MoO_3 is deposited followed by the ‘diluted donor’ active layer comprising 50nm of C_{60} (CreaPhys GmbH) doped with 6mol% (~5wt%) of each donor molecule. Afterwards, 8nm of bathophenanthroline (BPhen), used as electron contact, is evaporated and finished with 100nm of Al. All the organic materials were purified by 2-3 times of sublimation. The device area is defined by the geometrical overlap of the bottom and the top contact and equals 6.44mm^2 . To avoid exposure to ambient conditions, the organic part of the device was covered by a small glass substrate glued on top.

The solution processed devices were prepared as follows; First, a 45 nm thick film of poly(3,4-ethylenedioxythiophene):poly(styrenesulfonic acid) (PEDOT:PSS) CLEVIOS P VP Al 4083 from Heraeus was spin coated on an ITO covered glass substrate. After annealing for 10 min at $130\text{ }^\circ\text{C}$, the active layer was deposited from a chlorobenzene solution (25 mgmL^{-1} total concentration), by spin coating at 1500rpm. The device was completed by thermal sublimation of a low work function electron selective electrode comprising a Ca(3 nm)/Al(110 nm) combination. The solution processed solar cells had an active area of 9.2 mm^2 as determined by the areal overlap of the employed electrodes.

1.2 Temperature dependent EL and PL measurements

The solar cells were fixed and contacted with gold plated spring electrodes in a custom built cryostat from Cryovac GmbH employing a CTI-cryogenics cold head cooled by a closed cycle helium system. The inner (sample) volume of the cryostat is filled with Helium gas as thermal contact medium to assure an as accurate heat/cooling transfer as possible. A Lakeshore 332 temperature controller is employed with its two heater elements and temperature sensors placed directly above and below the sample. Measurements are only conducted when the sensors have been displaying equal temperatures for 15 minutes. The sample temperature certainty of this configuration employing contact gas is from our experience superior to standard vacuum cryostats where heat transfer and thermal equilibration is severely hampered. Electroluminescence is achieved by current injection of a defined sourced current (or voltage) by an Agilent 4155C parameter analyzer for 5-10 seconds during which the spectra are collected. Photoluminescence is provided by exciting the sample from the side widow with a defocused CW 405nm, 4.5mW CPS405 laser diode module from Thorlabs. The emission from the sample, originating from EL or

PL, is collected by a large lens mounted directly outside the cryostat at a distance of 3 cm from the sample thus collecting a majority portion of the emitted light. The collected light is focused on a 5.1 mm diameter liquid light guide coupled to a Ne calibrated Princeton Instrument Acton Spectra Pro SP2300 spectrometer equipped with a N₂ cooled Pylon 400 CCD detector. The entire beam path from the lenses to the detector was photon flux calibrated by a 45 W standard irradiance quartz halogen tungsten source from Newport (Oriel part 63358) certified at NIST (USA). The presented temperature dependent measurements on various sets of OPV samples have been collected during an extended time period between 2014 and 2019.

1.3 Measurement conditions and precautions

Samples with very low radiative efficiencies, such as CT emission ($\sim 10^{-6}$), mounted in insulating high vacuum sample compartments, and excited with strong laser light intensities or high injection currents, are unlikely to internally retain the indicated temperature of the temperature controller, usually mounted in a position slightly away from the sample under test. Here we use He filled sample chambers to assure excellent thermal contact between the sample and the temperature of the environment inside the cryostat, which is measured by two temperature sensors mounted slightly above and slightly below the sample. Although the He contact gas provides a substantially improved condition compared to simple vacuum cryostats used in several of the referenced studies, it does still not guarantee that also the internal temperature of the illuminated sample equals that stated by the temperature sensor. To even further approach optimized thermal conditions we therefore use only weak injection for electroluminescence and we employ a defocused laser spot size, providing a 405nm CW photon flux of $1.3E17 \text{ s}^{-1}\text{cm}^{-2}$ for photoluminescence, corresponding to approximately one quarter of the solar photon flux.

For fair comparison of the temperature dependent electroluminescence spectra, the measurements should at best be conducted by injection of carriers in either constant current or constant voltage mode. The large temperature range we strive for however generally prevents the constant voltage mode to be fulfilled entirely, as measurements at low voltages and low temperatures does not lead to any detectable emission, whereas a high voltage at high temperature inject far too much current and may easily heat and even burn the device. We have therefore preferred the constant current mode for a majority of our devices and in each graph it is specified which injection current has been employed.

An accurate temperature certainty and preclusion of device heating can nonetheless not be fully guaranteed. However, as the diluted donor OPV configuration mostly comprises C₆₀ molecules it offers us a great advantage in terms of also assuring the internal temperature of the device, as the high energy vibrations of the C₆₀ molecules become pronounced only at temperatures below 80K³²⁻³⁵. In our bulk heterojunction, the high-energy vibrational modes of the fullerene are again manifested from the pure phases of C₆₀ as a clearly structured and typical low temperature emission spectra. The appearance of these peaks in figure 4A of the main manuscript is thus our most solid insurance that we indeed reach and safely measure at the sought-after low internal device temperatures.

2. Supplemental data of voltage independent line-widths

We here present a few examples of CT-state electroluminescence from complete devices as a function of applied external voltage/injection current density. As outlined in the introduction of the main text, in case of substantial static exponential tail disorder, it is expected that the emission peak should blue shift with

higher voltages/injection currents. In **Figure S1**, the normalized EL spectra of the 4 different material systems are shown at different applied external voltages. Due to the employment of the sensitive detection system in conjunction with an optimized light collection from the cryostat, we are able to evaluate a majority of our devices at relatively low injection currents and voltages, often in the exponential (diffusion governed) part of the I-V curve. This does not only reduce parasitic joule heating of the device as outlined above, but also minimizes the population of conceivable pure material phases present in the active layer, which clearly was a greater concern previously, and apparently also the case in the work by Kahle *et al.* The most relevant observation of figure S1 is however that three of the four devices show insignificant peak-shift with increased injection current, even when our applied voltage exceeds the energy corresponding to the optical gap of the pure materials. The polymer-based cell however do show a minor (but still very small) blue shift upon increased voltage. These observations are therefore in accordance with the earlier observations by Gong *et al.*¹² supporting that static disorder defined by an exponential DOS tail is not dictating the spectral line-width of emission from the OPV material blends.

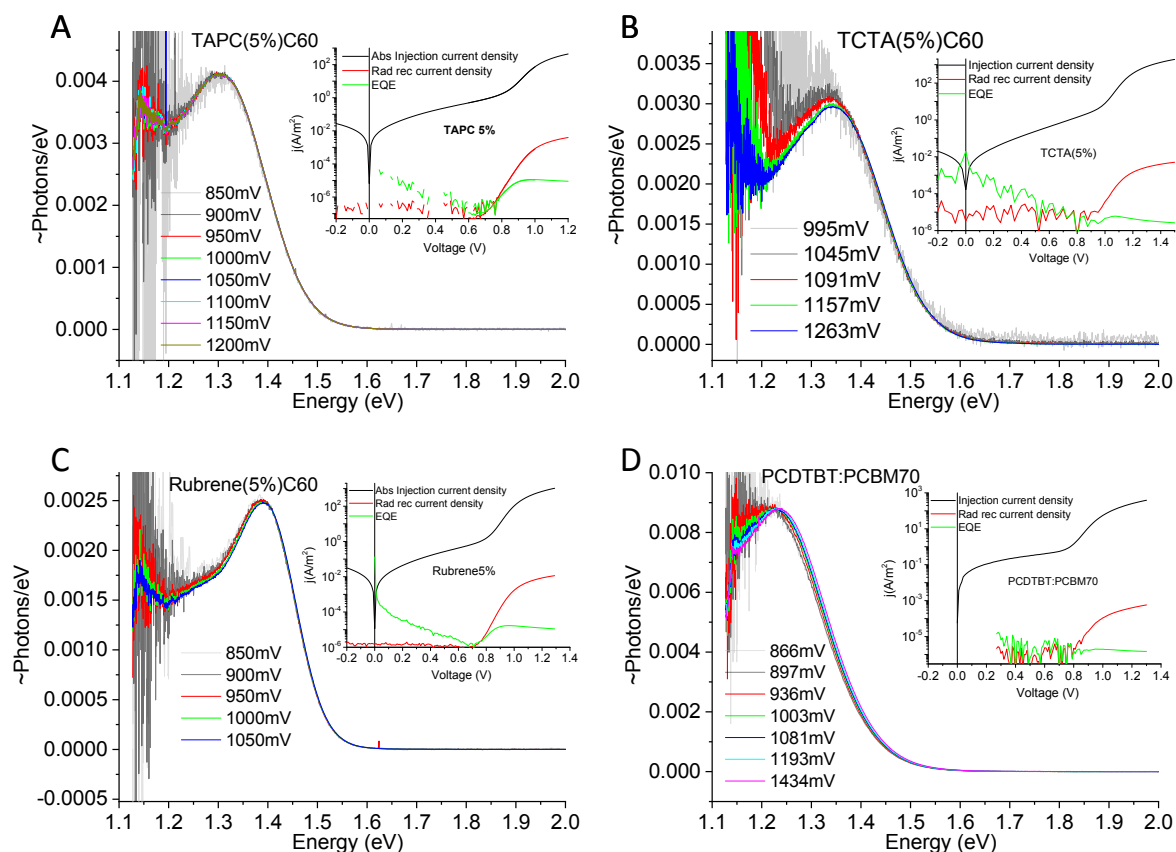


Figure S1. Voltage dependence at 294K of the four evaluated samples in the main manuscript. Inset shows the injection current, radiative recombination current and the derived EQE of emission as a function of voltage.

Figure S2 further supplements figure S1 with additional voltage dependency of TAPC(5%)C60 evaluated also at two selected lower temperatures.

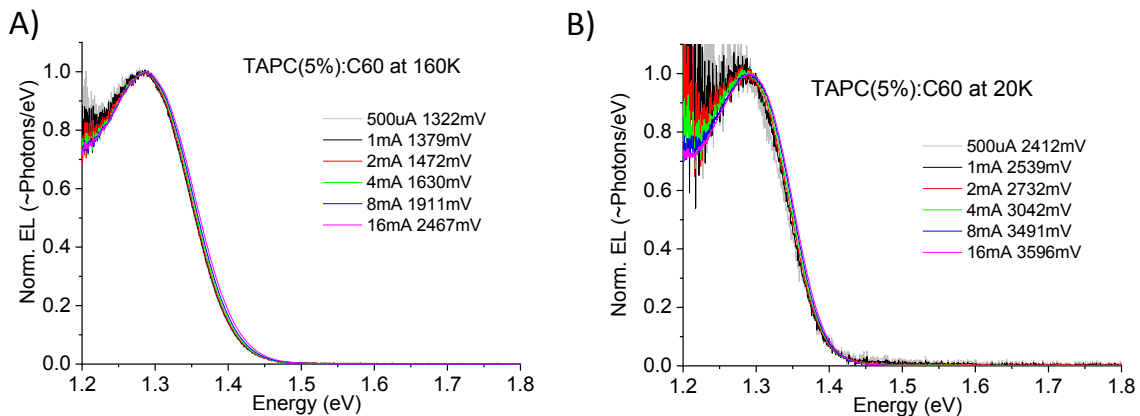


Figure S2. Injection dependence of the EL of TAPC(5%): C₆₀ at (A) T = 160 K and (B) T = 20 K. The injection (voltage) independence largely prevails also at reduced temperatures.

3. Supplemental data of temperature dependent line-widths of more materials

To solidify the generality of the claims made in the main manuscript we include EL(T) spectra of more materials that were measured earlier (2014-2016). At that time, we did not care sufficiently about the lowest temperature measurements, and they are accordingly not available for these materials. The clear confirmation of CT-state line-width narrowing upon cooling follows the classical description in the evaluated high temperature regime for the three OPV blends in panel A, B and C. The pure MDMO-PPV device in D shows on the contrary an exponential high-energy tail that mostly appears to redshift with cooling.

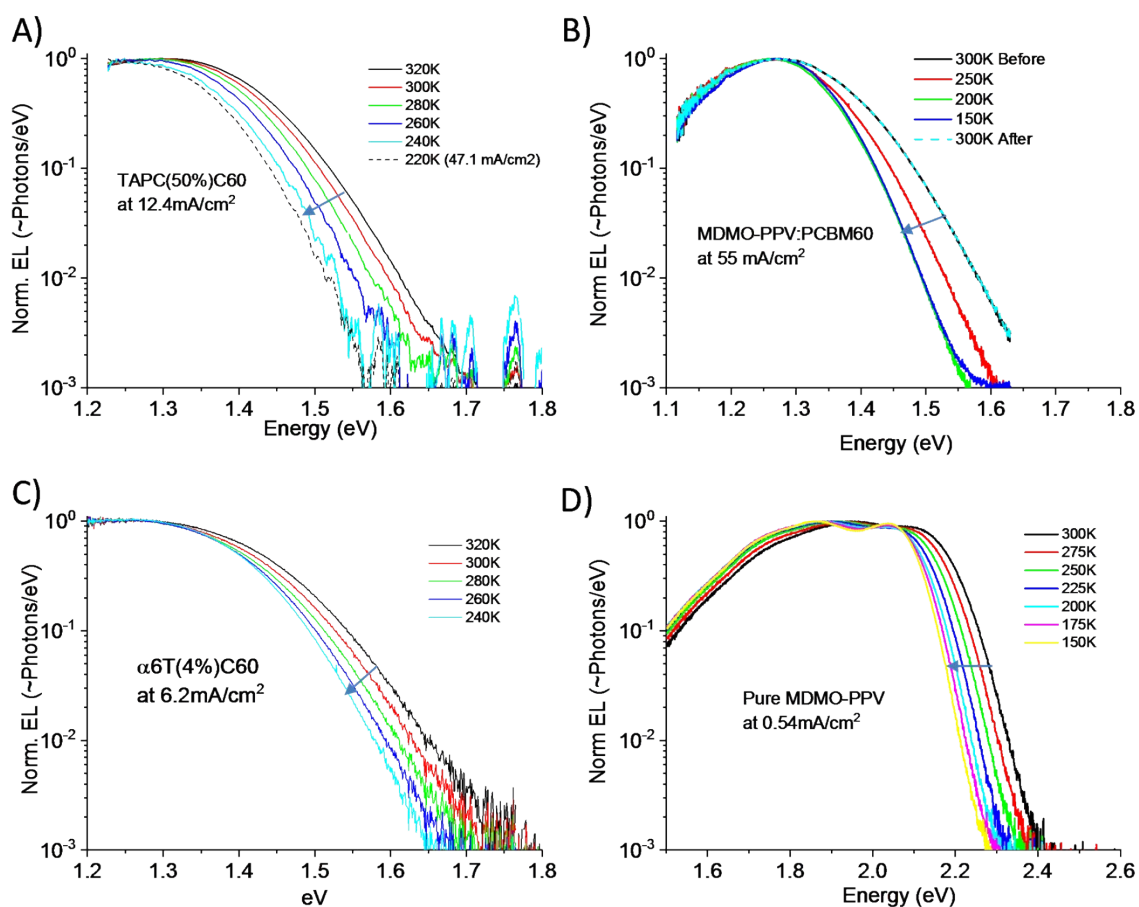


Figure S3. Temperature dependence of the line-width broadening for three additional earlier (2014-2016) evaluated organic solar cells (A-C). Here, the studied temperature range was smaller as compared to the new material set in the main manuscript. Figure D shows the T-evolution of a pure MDMO-PPV (a bad OLED) device displaying mostly a redshift of the exponential high-energy emission tail.

4. Studied materials

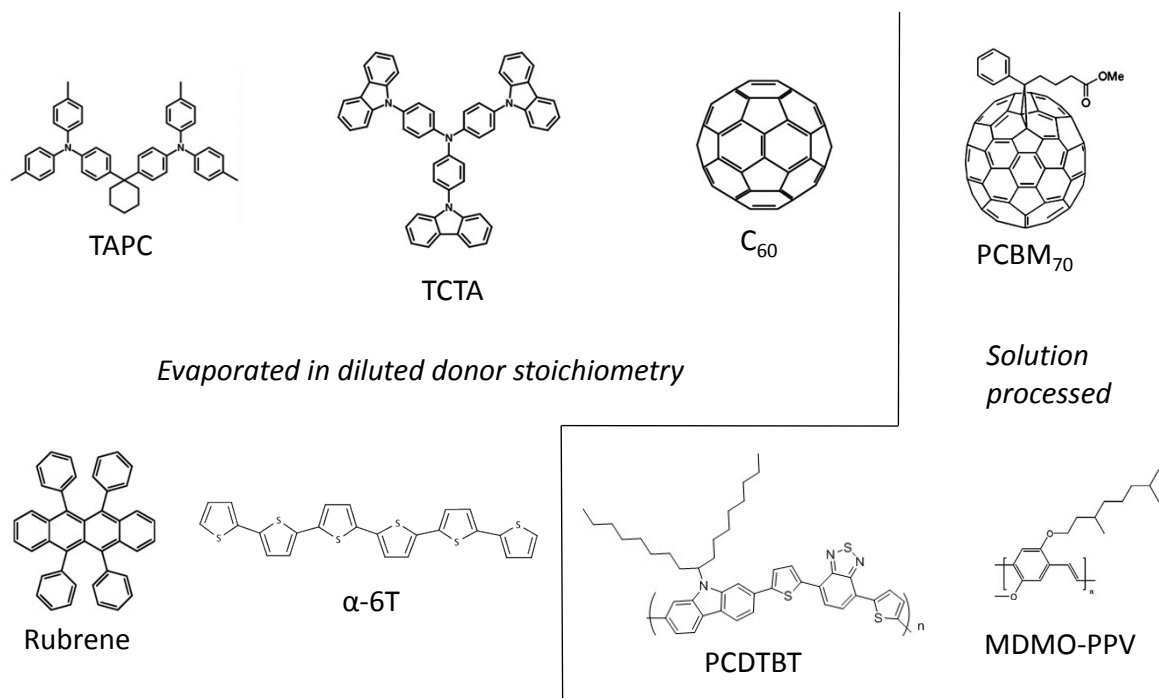


Figure S4. Molecular structures of the herein studied materials.